# 15

# Field Measurement of Hydraulic Conductivity of Rocks

Maria Clementina Caputo and Lorenzo De Carlo
*Water Research Institute (IRSA), National Research Council (CNR)*
*Via F. De Blasio, Bari*
*Italy*

## 1. Introduction

Groundwater often represents the main and most precious source of drinking water supply for the population. In recent decades, overexploitation, uncontrolled anthropogenic actions and continuous reduction of rainfall, due to climate change, led to a depletion of the water resource by affecting both its quantity and quality. The scientific community pays attention to this particular environmental issue in order to implement effective strategies for the safeguarding, protection, and remediation of the aquifers. Over the last decade, considerable efforts have been made to develop methodologies and techniques aimed at improving knowledge of the processes that are based in the unsaturated zone or vadose zone—the portion of the soil above the groundwater level—within which flow and transport processes occur. In this portion of subsoil, in fact, important physicochemical phenomena take place, which regulate the environmental balance of the hydrogeological system, such as the ability to store water and transport it into the ground below. It also has a natural protective function as a filter for any potential pollutants carried by fluids circulating in the solid matrix before reaching the groundwater. The knowledge and the understanding of the processes that take place in the unsaturated zone are, therefore, essential for groundwater management and protection, to evaluate the recharge rate and assess groundwater vulnerability. In particular, the measurement and monitoring of the unsaturated hydraulic properties are very important, even though it is difficult and expensive (Castiglione et al., 2005). The methods and techniques developed are designed to investigate the unsaturated flow process in the soils. When the vadose zone consists of rock, rather than soil, technical aspects increase the difficulties in several ways (Bogena et al., 2007; Kizito et al., 2008). Usually, different kinds of probes are used to monitor the water infiltration in soils: the Time Domain Reflectometry (TDR) (Jones et al., 2004; Robinson et al., 2003), the Frequency Domain Reflectometry (FDR) and multi-sensor capacitance probes (Baumhardt et al., 2000; Seyfried et al., 2004) are used to measure the water content in the subsurface, while tensiometers measure water pressure (Masbrucha & Ferré, 2003). These devices are hard to utilize in the rocks, mainly because the probes are brittle. Therefore it is difficult to install them, as there needs to be good contact between the rock and the sensor to reduce the uncertainty of the measurements due to the gap effects. Field studies, set up to measure hydraulic conductivity, have employed infiltrometer tests under different conditions, but they have rarely been performed directly on the outcropped rock, owing to the difficulty of

installation. Reynolds et al. (2002) conducted infiltrometer tests under different conditions, Ledds-Harrison & Youngs (1994) used very small diameter rings (from 1.45 mm to 2.5 mm) for field measurements on individual soil aggregates, Youngs et al. (1996) used a 20 m diameter infiltrometer cylinder to measure highly structured and variable materials that could not be sampled adequately by a smaller cylinder. Castiglione et al. (2005) developed in the laboratory a tension infiltrometer ring, 4 cm in height and 27.5 cm in diameter, suitable for accurate measurements of infiltration into a big sample of fractured volcanic tuff, at very low flow rates over long equilibration times. Most field studies employ cylinder infiltrometers with diameters ranging commonly from 1 to 50 cm, which are poorly representative of the heterogeneous media, such as fractured rocks, in which hydraulically important fractures may, typically, be spaced further apart than the cylinder's diameter. Indeed, up to now infiltrometer tests have rarely been performed directly on-site on rock outcrops. This chapter describes a methodology to obtain the field-saturated hydraulic conductivity, $K_{fs}$, by using a ring infiltrometer, with a large (~2 m) adjustable diameter, developed for measuring quasi-steady infiltration rates on outcropped rock. $K_{fs}$ is the hydraulic conductivity of the medium (soil or rock) when it has been brought to a near-saturated state by water applied abundantly at the land surface, typically by processes such as ponded infiltration, copious rainfall or irrigation. The proposed device is inexpensive and simple to implement, as well as very versatile, owing to its large adjustable diameter that can be fixed on-site. Moreover, certain practical problems, related to the installation of the cylindrical ring on the rock surface, were solved in order to achieve a continuous and impermeable joint surface between the rock and the ring wall. An issue of major concern is linked to the edge effects, related to the radial spreading of the infiltrating water; obviously smaller rings are more influenced by these effects. Swartzendruber & Olson (1961) and Lai & Ren (2007) found that the ring infiltrometer needs a diameter greater than 1.2 m and 0.8 m, respectively, to avoid the edge effects. For this reason, the proposed large ring infiltrometer is made of a strip of flexible material with which build the cylinder on-site, with a suitable diameter in relation to the lithological and topographical features of the field. The flexible material, such as plastic or glass resin, allows the minimization of the size of the ring and, therefore, its movement easily, in order to acquire a large number of independent $K_{fs}$ measurements over a given area. In fact, because of the extreme spatial variability of $K_{fs}$, its value finds statistical consistency in multiple tests. Geophysical techniques were coupled with the infiltrometer tests in order to monitor, qualitatively, the water infiltration depth, to allow a rapid visualization of the change in water content in subsurface and to ensure that the decrease in the water level in the ring was caused mainly by vertical water infiltration, and not by the lateral diversion of water flow. Since the late 1980s, many geophysical applications have been aimed at hydrogeological studies. White (1988) conducted electrical prospecting to determine the direction and the flow rate of saline aquifers using a tracer. Daily et al. (1992) used borehole electrical resistivity surveys to obtain the distribution of electrical resistivity in the subsurface, and compare the results with infiltrometer tests. Recently, electrical resistivity techniques have been used to monitor hydrogeological processes. Cassiani et al. (2006) conducted a monitoring test of a salt tracer by means of the application of electrical resistivity tomography using a time-lapse technique. The movement of the tracer was monitored with geophysical images. The methodology described in this chapter was carried out on different lithotypes in order to verify the applicability of the experimental apparatus in very different geological conditions. In particular two cases are described: the Altamura test site that represents a case of hard sedimentary rock consisting

of limestone, and the San Pancrazio test site as an example of a soft porous rock, specifically calcarenite. Both sites, located in the Puglia region of southern Italy, have been studied because they are both contaminated areas, for which the understanding of the flow rate in the subsurface is very important in order to design a remediation strategy. The experimental approach gave good results in both situations that mean it could be used successfully on each different lithology of outcropped rock.

## 2. Method

The objective of this chapter is to describe a methodology to obtain the field-saturated hydraulic conductivity, using a large ring infiltrometer installed directly on the outcropped rock. The method considers an integrated approach that combines the infiltrometer test with geophysical techniques, in order to visualize the change in water content in the subsurface during the experiment. Among geophysical techniques, we have used electrical resistivity images (ERI) because the electrical resistivity is extremely sensitive to subsurface water content. Moreover, electrical time-lapse resistivity measurements (Binley et al., 2002; Deiana et al., 2007), carried out simultaneously with the infiltrometer test, allow us to check the performance of the experimental apparatus and, particularly, that the decrease of water level in the ring is due to the infiltration and not to the losses along the edge of the ring.

### 2.1 Large ring infiltrometer

A ring infiltrometer for studying water flow in rock formations needs to be made from a tough material, suitable for installation on the rock surface. At the same time, the material must be both flexible, to allow a cylinder to be built that is adjustable to the field conditions, and light, to facilitate transport and setup. Where the ground surface is very irregular, small adjustments to the ring diameter ensure efficient sealing, thus facilitating the setting-up of the device. If electrical methods are to be used for the detection of water content or salinity, the ring must also be made of a non-metallic material. The large ring infiltrometer was, therefore, designed in a light and flexible material, such as plastic or glass resin, to allow easy installation on the rock surface, and the adaptation of its size to the field conditions. Strips of the flexible material 30 cm wide and 0.2 cm thick were used to build in-situ rings of internal diameter of about 2 m, by sealing the two ends of the strip with impermeable adhesive tape to form the cylinder. The large diameter provides infiltration data that are representative both of the anisotropy and the heterogeneity of the rock, characteristics which cannot be sampled adequately by using smaller rings. It thus allows an improved representation of the natural system's heterogeneity, while also taking into consideration irregularities in the soil/rock subsurface. In addition, the large diameter allows the avoidance of the edge effects that usually occur during infiltration, such as the radial spreading of the infiltration water. Among a variety of materials tested to seal the ring to the ground, both in the laboratory and in the field, gypsum was shown to be the most suitable because it is cheap, easy to prepare in situ and to apply on the ground in a previously hollowed furrow, ensuring good sealing. Clay, instead, needed to be worked for a long time in order to obtain a consistency that would allow the ring to be sealed to the ground. It nevertheless gave poor results, because the clay did not grip the ring wall firmly on the ground. Moreover, tests carried out with clay at the laboratory showed water losses from cracks in the clay due to its characteristics of swelling and shrinking. Silicon was also tested, although using it for sealing a large-diameter infiltrometer would be expensive. However, it

was also discarded, as it did not seal well due to the dissimilarity of the soil, rock, and plastic materials being sealed. Polyurethane foam was easy to apply and proved impermeable, but was also discarded because it was expensive and did not grip well on the rock and/or soil.

### 2.2 Geophysical techniques

Geophysical techniques are used routinely for subsurface investigation, as they provide information about the physical properties related to geological and hydrogeological conditions. There are two main groups of geophysical methods: the active methods, which measure the subsurface response to electromagnetic, electrical, and seismic artificially generated signals; and the passive methods, which measure the earth's natural fields, such as the magnetic, electrical, and gravitational ones. Among these, the electrical resistivity method is a relatively new imaging tool in geophysics; it is an active method that determines the subsurface distribution of electrical resistivity from a large number of resistance measurements. The electrical resistivity, ρ, is an intrinsic property of rock and soil, and is a measure of how strongly a material opposes the flow of electric current. The direct current resistivity tomography method considers spatial variations in electrical resistivity among geologic materials for mapping the subsurface structures. It is used extensively in the search for suitable groundwater sources, and also to monitor types of groundwater pollution. In engineering it is used to locate subsurface cavities, faults and fissures, permafrost, mineshafts etc., and in archaeology, for mapping out the areal extent of the remnants of buried foundations of ancient buildings, and many other applications (Reynolds, 1998). The electrical resistivity method is based on the Ohm's laws; the first of which states that when the electrical current, I (ampere, symbol A), passes through an electrically uniform medium of side length, L (m), the material has a resistance, R (ohm, symbol Ω), resulting in a potential drop, V (volt, symbol V), between opposite faces of the medium. The first Ohm's law correlates the three physical parameters into the formula:

$$V = RI \tag{1}$$

The resistance, R, is proportional to the length, L, of the resistive material and inversely proportional to the cross-sectional area, S ($m^2$) (second Ohm's law)

$$\rho = \frac{RS}{L} \tag{2}$$

where ρ is the electrical resistivity (ohm x m, symbol Ωm); it is the inverse of the conductivity (siemens/m, symbol S/m).

Electrical current can flow in rocks and soils by three main mechanisms: 1) electrolytic conduction that occurs by means slow migration of ions in a fluid electrolyte, controlled by ions type, ion concentration, and ionic mobility; 2) electronic conduction that occurs in metals through rapid movement of electrons; 3) dielectric conduction that occurs in conducting materials, or insulators, in the presence of an external alternating current when atomic electrons are shifted slightly relative to the nucleus. In most rocks, electrical current flows by electrolytic conduction (Telford et al., 1990). The electrical resistivity of the soils and rocks correlates with other soil/rock properties which are of interest to the geologist, hydrogeologist, and geotechnical engineer. Many factors affect electrical resistivity, such as

texture, porosity, water saturation, clay content, permeability and temperature. Thus, the resistivity measurements cannot be related directly to the type of soil or rock in the subsurface without direct sampling, or some other geophysical or geotechnical information. Porosity is the major controlling factor of the changing resistivity of the rock, because the electricity flows in the near surface by means of the passage of ions through the pore space of the subsurface materials. The porosity (amount of pore space), the permeability (connectivity of pores), the water (or other fluid) content in the pores, and the presence of salts all are contributing factors to changing resistivity. Archie (1942) developed the empirical formula of the effective resistivity of the rock, $\rho_e$:

$$\rho_e = \rho_w a \varphi^{-m} S^{-k} \tag{3}$$

where φ (%) is the porosity, S (adimensional) is the volume fraction of pores with water, $\rho_w$ is resistivity of pore fluid, a, m and k are physical parameters. $\rho_w$ is influenced by dissolved salts and can vary between 0.05 Ωm for saline groundwater, up to 1,000 $\Omega m$, for glacial melt water. Archie's law ignores the effect of pore geometry, but it is a reasonable approximation for many sedimentary rocks.

### 2.2.1 Electrical resistivity imaging

The technique of electrical resistivity imaging utilizes measurements of electrical potential associated with the subsurface electrical current flow, generated by a direct current. In the electrical resistivity method, the spatial variation of resistivity in the field is determined using four electrode measurements, and is based on measuring the potential difference between one electrode pair while another electrode pair, used as the current source, transmits the current (Dahlin, 2001). Measurements of the potential difference between the two electrodes allow the determination of the apparent resistivity, $\rho_a$:

$$\rho_a = \frac{K \Delta V}{I} \tag{4}$$

where K (m) is a geometric factor depending on the used array. The measured quantity is called apparent resistivity because the resistivity values measured are averages over the total current path length, but are plotted at one point for each potential electrode pair. The data can be arranged in a 2-D plot, called pseudosection, which displays both horizontal and vertical variations in apparent resistivity. The conventional presentation places each measured value at the intersection of two 45-degree lines through the centres of the dipoles (Edwards, 1977). The interpretation of the resistivity data consists of two steps: a physical interpretation of the measured data, by means of an inversion process that results in a physical model; and a geological interpretation of the resulting physical parameters (Dahlin, 1996). Many configurations of array can be used for measuring the distribution of electrical resistivity of the subsurface. The arrays most commonly used for 2-D imaging surveys are: Wenner, dipole-dipole, Wenner-Schlumberger. The choice of the best array considered for the surveys, depends on the depth of investigation, the sensitivity of the array to vertical and horizontal changes in the subsurface resistivity, the horizontal data coverage, and the signal strength (Loke, 2001). In general, Wenner array is relatively sensitive to vertical changes in the subsurface resistivity, but it is less sensitive to its horizontal changes. It is useful for recognized horizontal structures (vertical

resistivity changes), but relatively poor in detecting narrow vertical structures (horizontal resistivity changes). Dipole-dipole is good for mapping vertical structures, such as dykes and cavities, but relatively poor for mapping the horizontal structures such as sedimentary layers or water table. Wenner-Schlumberger is moderately sensitive to both horizontal and vertical structures. In areas where both types of geological structures are expected, this array might be a good compromise between the Wenner and the dipole-dipole array.

## 3. Field tests

The infiltration experiments described in the chapter refer to two sites that differ in their geological and hydrogeological conditions, in order to show how the methodology can be applied widely. The sites consist of outcrop of hard sedimentary rock, fractured limestone, in the case of Altamura, and soft sedimentary rock, in the case of San Pancrazio (Fig. 1). The different lithology implies different infiltration process and, consequently, different experimental approaches and interpretations of the experimental data. All these aspects are described in detail for each test site.

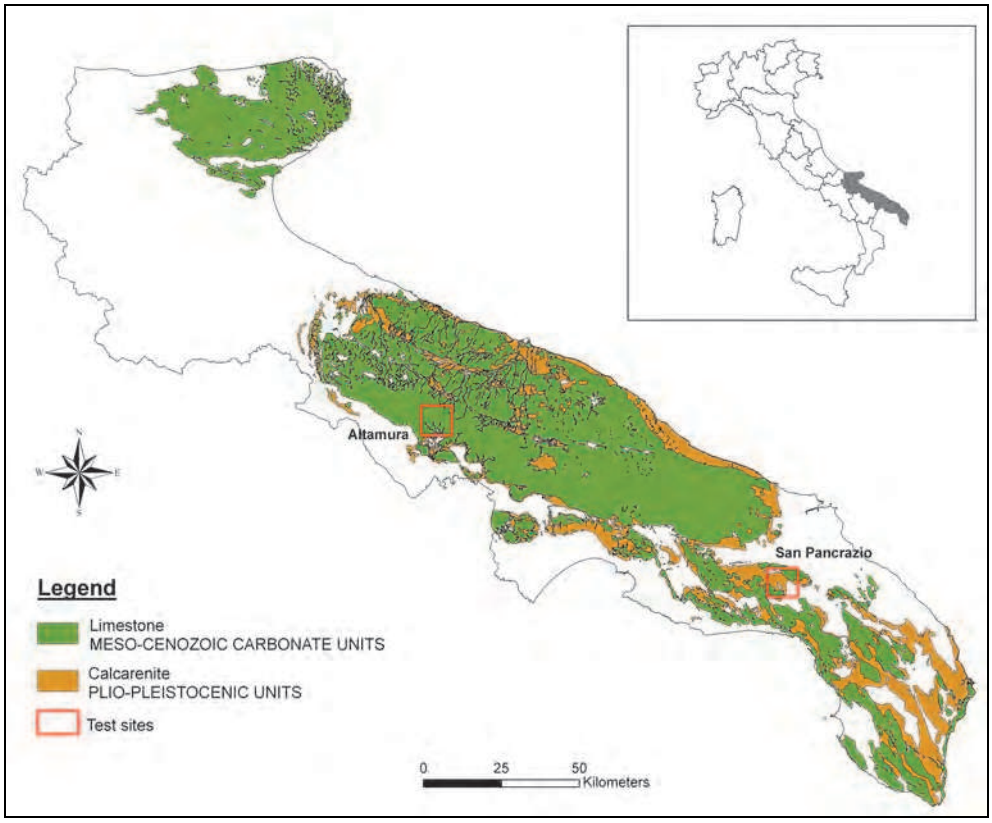


Fig. 1. Schematic geological map of the Puglia region.

### 3.1 Test on limestone

The infiltration experiments were performed in the study area belonging to Altamura territory, located in southern Italy (Fig. 1). The site is part of the Murge plateau, formed from Cretaceous limestone during the Paleogene and Neogene periods. The limestone is part of a sedimentary sequence of a carbonatic platform some thousands (up to 3,000) of meters thick. The main rock units consist of calcilutites, which in the study area constitute a unit known as "*Calcare di Altamura*" and "*Calcare di Bari*" (Ciaranfi et al. 1988). During a large part of the Neogene, the area was uplifted and affected by tectonic stress and karst morphogenesis. The experimental tests were conducted on the top of a karstic fractured limestone formation constituting the deep Murge aquifer, which has a water table ranging in depth from 400 to 500 m below the ground surface. The fractured limestone studied is characterized by low effective matrix porosity with respect to fracture porosity. Borgia et al. (2002) measured the effective matrix porosity of the limestone, at field scale, and found values up to 0.1%, together with a permeability lower than 24 mD (millidarcy), and a hydraulic conductivity of $2.1 \times 10^{-2}$ m $d^{-1}$ (for water at 20°C), on average. These values indicate a conductivity 1,000 times lower than that of the fracture network (8–77 m $d^{-1}$) of the same limestone formation (Masciopinto, 2005), which is characterized by an effective fracture porosity at field scale of up to 0.4% (Borgia et al., 2002). In light of these results, it is clear that the water flow rate component in the rock matrix can be considered negligible as compared to the water flow rate component in the network of fractures. This site was chosen for testing the newly developed large ring infiltrometers because it was affected by untreated sludge waste deposits that have caused soil and rock contamination by heavy metals (chromium, lead, zinc, nickel and cadmium), as well as hydrocarbons. Several soil chemical analyses carried out, showed chromium and nickel contamination, with concentrations higher than both Italian and European legal limits. The infiltrometer tests were carried out at two locations, 300 m apart, to evaluate the quasi-steady vertical flow rates in outcrops of limestone that showed different fracture frequencies and sizes on visual inspection. Specifically, the site of test #1 showed prominent visible fractures of about 5 cm spacing and about 1 mm aperture, whereas the site of test #2 showed no visible fractures (Fig. 2). A 2 m diameter ring, coupled with an external ring, was used in test #1. In this case, the infiltration area consisted of a central part with numerous visible fractures (Fig. 2a), while the rest was partially covered by soil, 5–10 cm thick, on average. For this reason, at this site, a second ring with a larger diameter (2.2 m) was positioned (Fig. 2b), in order to improve the hydraulic packing during the water infiltration test. Continuity between the ring infiltrometer wall and the rock-soil surface was obtained by filling the space between the external and internal rings with gypsum, up to a height of about 2 cm, to create a seal.

As a result, the second ring improved the gypsum sealing of the first ring to the ground, overcoming the challenge presented by the presence of different media (rock and soil) along the edge of the ring. In the second test (#2), located in an area with an outcrop of limestone characterized by no visible fractures, a 1.8 m diameter ring was inserted into a thin furrow 2 cm deep, previously hollowed into the rock (Fig. 3), which was then also sealed with gypsum. In both tests, the large diameter ring allowed the obtaining of data more representative of the anisotropy and heterogeneity of rocks than those obtained with a small ring. The difference in size of the rings used in the two tests was due simply to the local field conditions; in fact, the device is designed to allow the diameter to be adjusted easily when the irregularity of the surface at the test site so requires. In both cases the infiltration tests have been supported by ERI, carried out simultaneously by means "time-lapse" technique,

in order to monitor the infiltration and redistribution of water in the subsurface. The water used for the infiltration test had moderate salinity (electrical conductivity of 2.39 mS/cm) to enhance the subsurface electrical resistivity measurements.

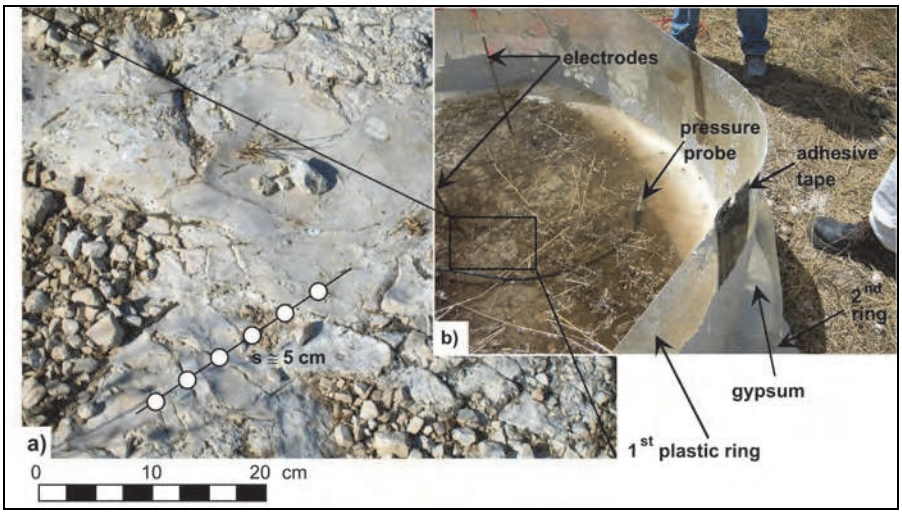


Fig. 2. Test # 1 at the Altamura site: a) fractured limestone with visible fractures of about 5 cm of spacing (s); b) plastic ring infiltrometer resting directly on the ground and sealed with gypsum by using a second ring.

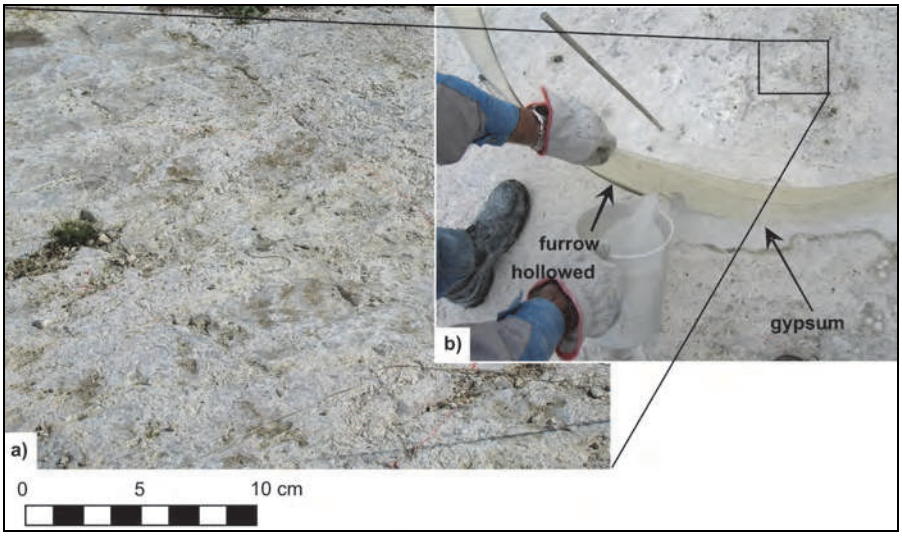


Fig. 3. Test # 2 at the Altamura site: a) limestone without visible fractures; b) plastic ring infiltrometer installed into a thin (2 cm) furrow hollowed in the limestone and sealed with gypsum.

In test #1, the resistivity data were collected using a 7.5 m long straight-line array of 16 steel electrodes with 0.5 m spacing, oriented in the parallel direction to the visible fractures. In test #2, two similar linear arrays were set up, perpendicular to each other, with the same length and electrode spacing, crossing at the center of the ring infiltrometer (Fig. 4.). The Wenner array was chosen over other array types because it provides a good signal-to-noise-ratio. Additionally, it is also highly sensitive to vertical changes in the subsurface resistivity. This makes the Wenner array a useful tool in studying the movement of the wetting front in time. The investigation depth is about 1.5 m, easily achievable with the chosen electrode configuration. Both tests used the IRIS–SYSCAL Pro Switch 48 instrument to acquire electrical resistivity measurements. To obtain 2-D resistivity models, the field data were inverted using Res2Dinv software (Griffiths & Barker, 1993; Loke & Barker, 1996). In the processing of resistivity data, an inversion routine based on the smoothness-constrained least-squares method was implemented (deGroot-Hedlin & Constable, 1990). The 2-D model used by the inversion program divides the subsurface into a number of rectangular blocks, whose arrangement is linked to the distribution of points in pseudosections. The distribution and size of the blocks is generated automatically by the program, using the distribution of the data points as a rough guide. The depth of the bottom row of blocks is set to be approximately equal to the equivalent depth of investigation (Edwards, 1977) of the data points. The optimization method basically tries to reduce the difference between the calculated and measured apparent resistivity values, by adjusting the resistivity of the model blocks. A forward modeling subroutine is used to calculate the apparent resistivity values, and a non-linear least-squares optimization technique is used for the inversion routine (Loke & Barker, 1996). A measure of this difference is given by the root-mean squared (RMS) error. However, the model with the lowest possible RMS error can sometimes show large and unrealistic variations in the model resistivity values, and might not always be the "best" model from a geological perspective. The water in the ring reached a maximum level of 0.13 m above the ground surface in both tests. During approximately 2 hours of the falling-head infiltrometer tests, the specific lateral water leakage fluxes were about 8% (0.1 m $d^{-1}$) and 3% (0.007 m $d^{-1}$) of the infiltrate water fluxes in the rings, for the first and second tests, respectively. The specific (i.e., per unit of ring area) leakage rates, due

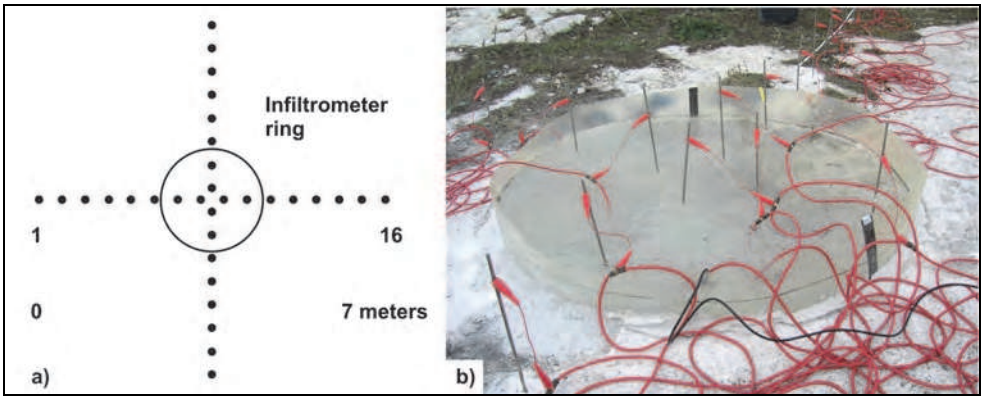


Fig. 4. Test # 2 at the Altamura site: a) scheme of electrode array; b) detail of field installation of electrodes.

not to the water flux from the edge of the ring (i.e., losses) but to the amount of infiltrated water which flowed laterally within the subsurface, was estimated by dividing the total water volume of the lateral diverted water flow by the duration of the infiltration (2 and 3.2 hours for tests #1 and #2, respectively). This estimation was performed on the basis of the areas of the wetted surfaces (1.6 and 1.5 m2 for tests 1# and 2#, respectively), which were observed around the rings at the end of each test, and multiplying them by the average thickness of the wetted layers (5 and 3 cm, respectively), and by their porosities (0.29 and 0.03) (Borgia et al. 2002). The thickness of the wetted layers was derived from measurements on core samples drilled at the test sites. During the experiments, water levels in the ring infiltrometer were monitored using a submersible pressure probe (PTX DRUCK LTD).

### 3.2 Test on calcarenite

The study area is an abandoned calcarenite open quarry, located near San Pancrazio city (Fig. 1). The quarry was used for about ten years, from 1980 to 1990, for the disposal of waste from a pharmaceutical company that produced antibiotics (in particular erythromycin), using fermentative processes and subsequent chemical transformations causing subsurface contamination. For this reason, field infiltrometer tests, coupled with electrical resistivity measurements, were carried out to evaluate the flow rate of potential contaminants in the porous aquifer. The geology of the study area consists of Cretaceous bedrock formed from dolomitic limestone and limestone, overlaid unconformably by Plio-Pleistocenic calcarenite. The oldest formations contain a deep and confined aquifer characterized by a potentiometric surface, ranging from 70 m to 80 m, in depth below ground surface. Electrical resistivity measurements have detected a shallow aquifer with a water table about 25 m below ground surface, and about 12 m below the bottom of the quarry in the Plio-Pleistocenic calcarenite. A large infiltrometer ring was installed in the field directly on the rock surface with an adaptable size to fit the condition in the field. A strip of 30 cm high flexible plastic material was used to build an in-situ infiltrometer ring, of about 2 m in diameter, sealing the two edges with impermeable tape. The ring was installed into a 5 cm deep thin furrow hollowed in the calcarenite at the bottom of the quarry, and sealed with gypsum (Fig. 5).

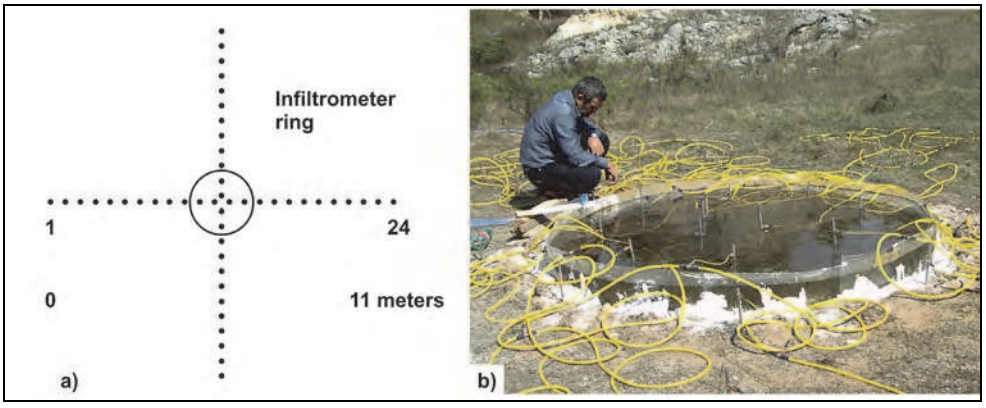


Fig. 5. Test at the San Pancrazio site: a) scheme of electrode array; b) detail of field installation of electrodes.

The infiltration tests were performed with constant and falling head conditions. About 0.27 $m^3$ of water was poured in the ring until the water level reached 8 cm from the bottom, and then another 0.2 $m^3$ to maintain that constant level in the ring for the duration of the test, which took 3 hours. No more water was added for the falling-head test because it started from the constant water level considered for the first test (under constant head condition). The second test took 2.5 hours. In order to study the infiltration/redistribution of water in the subsurface, electrical resistivity tomography was carried out simultaneously with the infiltrometer tests by collecting resistivity data along two electrical profiles, each of which was 11.5 m long, with 24 steel electrodes with 0.5 m spacing. The two electrical profiles were set up, perpendicular to each other, with the same length and the same electrode spacing for each direction (x, y), and in a symmetrical position with respect to the center of the ring infiltrometer (Fig. 5). The so-called Wenner array was chosen as at the Altamura test site. The same instrument resistivity meter, IRIS–SYSCAL Switch Pro 48, was used to measure the resistivity of the subsurface. During the infiltrometer tests, the monitoring of the infiltrated water was carried out by means of a time-lapse technique, collecting more than 2,000 measurements for each acquisition. The total acquisition time was about 3 hours for the constant head test, and about 2.5 hours for the falling head test.

## 4. Results

In the following paragraphs the results related to the two different test sites are described: the Altamura site consisting of limestone with and without visible fractures, such as an example of hard sedimentary rock, and the San Pancrazio site consisting of calcarenite, such as an example of soft sedimentary rock. Different approaches are used for the elaboration of the experimental data collected at the two geological outcrops. It is highlighted that in the case of fractured limestone the interpretation of the data collected experimentally, needs a numerical elaboration supported by mathematical models.

### 4.1 Limestone

The results of the infiltrometer tests are summarized in the graph in Figure 6, which shows a constant decrease in the water level in the ring during the tests, after the water level had reached its maximum depth of 0.13 m in both cases. The slope of the trend line of experimental sites gives an average infiltration rate equal to 1.33±0.0034 m $d^{-1}$ for test #1, and 0.22±0.0027 m $d^{-1}$ for test #2, where the standard deviations take into account the standard errors of the best fit procedures. In order to interpret the results of the falling head infiltrometer test, the simplified equation from Nimmo et al. (2009) was considered:

$$K_{fs} = \frac{L_G}{t} \ln\left(\frac{L_G + \lambda + D_o}{L_G + \lambda + D}\right) \tag{5}$$

where $K_{fs}$ ($LT^{-1}$) is the field-saturated hydraulic conductivity, t is the time, $D_o$ and D are the initial and final ponded depths, respectively, $L_G = C_1 d + C_2 b$ is the ring-installation scaling length, with 0.993 and 0.578 as recommended values for $C_1$ and $C_2$, while d and b are the ring insertion depth and ring radius, respectively, and λ is an index of how strongly water is driven by capillary forces in a particular medium. The macroscopic capillary length, λ, during downward water movement in a fracture plane, is related to the fracture aperture and the interfacial surface tension $\sigma$ ($M/T^2$) between air and water (equal to 71.97 dyn/cm

at 25°C) (de Gennes et al., 2002), using the following Young-Laplace equation (Pruess & Tsang, 1990):

$$\lambda = 2\frac{\sigma}{\rho g \times \bar{b}_c} \tag{6}$$

assuming that the water-air contact angle equals zero, and that the cutoff aperture, $\bar{b}_c$, equals the fracture aperture which delimits the region occupied only by the non-wetting phase, $g$ (L/t²) is the gravity acceleration and $\rho$ (M/L³) is the water density. In order to estimate the field-saturated hydraulic conductivity value, Kfs, by means of equation (5), the macroscopic capillary length, λ, is required. It is determined by inverse modeling, using an unsaturated fractured flow model in the vertical 2-D fracture (Masciopinto & Benedini, 1999). The model solutions were then calibrated on the basis of the comparison between the shapes of the wetting front obtained from the simulation outputs and those of the electrical resistivity images at the correspondent time (Figs. 7 - 8). After estimating the macroscopic capillary length (0.90 m and 0.95 m for tests #1 and #2, respectively) and the corresponding cutoff aperture (16.5 μm and 15.5 μm), equation (5) gave field-saturated conductivity values of 0.67±0.01 m d$^{-1}$ and 0.054±0.001 m d$^{-1}$ for tests #1 and #2, respectively.

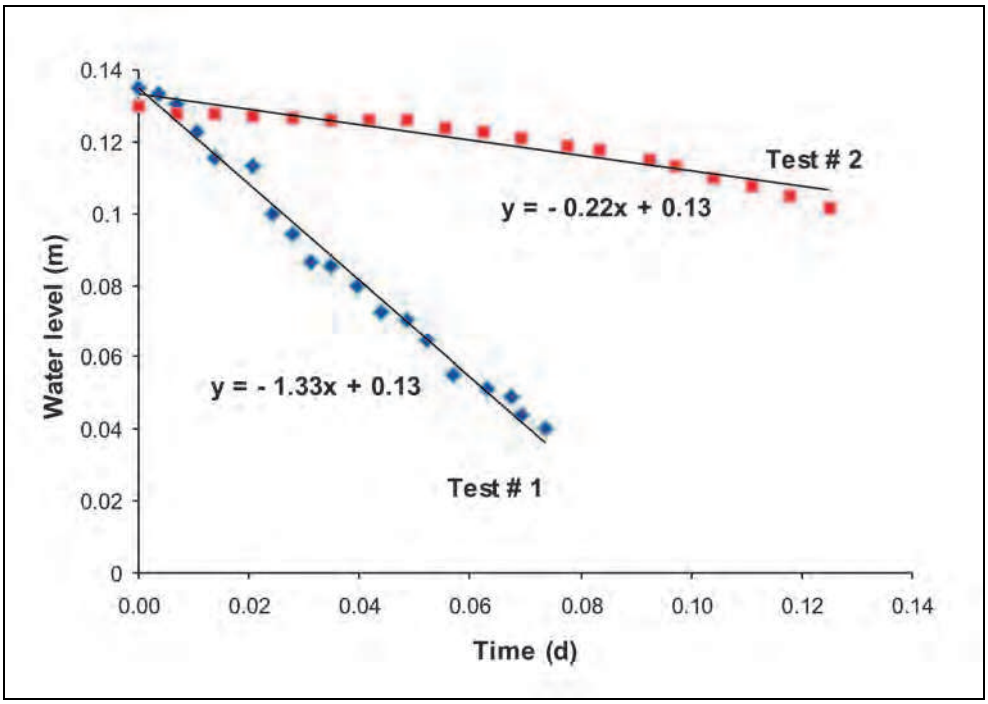


Fig. 6. Measured water level versus time during tests # 1 and #2 at the Altamura site.

The notable difference between the field-saturated hydraulic conductivity values of tests #1 and #2 highlights the great variability in hydraulic properties which characterizes the carbonate rocks studied. In fact, even though the two test sites were only 300 m apart, and

the experiments were performed on the same geological formations, the infiltration rates observed in the areas tested were very different. For the Altamura fractured limestone, the modified Kozeny-Carman equation (Pape et al., 1999) leads to outcrop saturated conductivity values ranging from 0.6 m $d^{-1}$ to 12 m $d^{-1}$, considering the rock outcrop porosity from 1% to 2%.

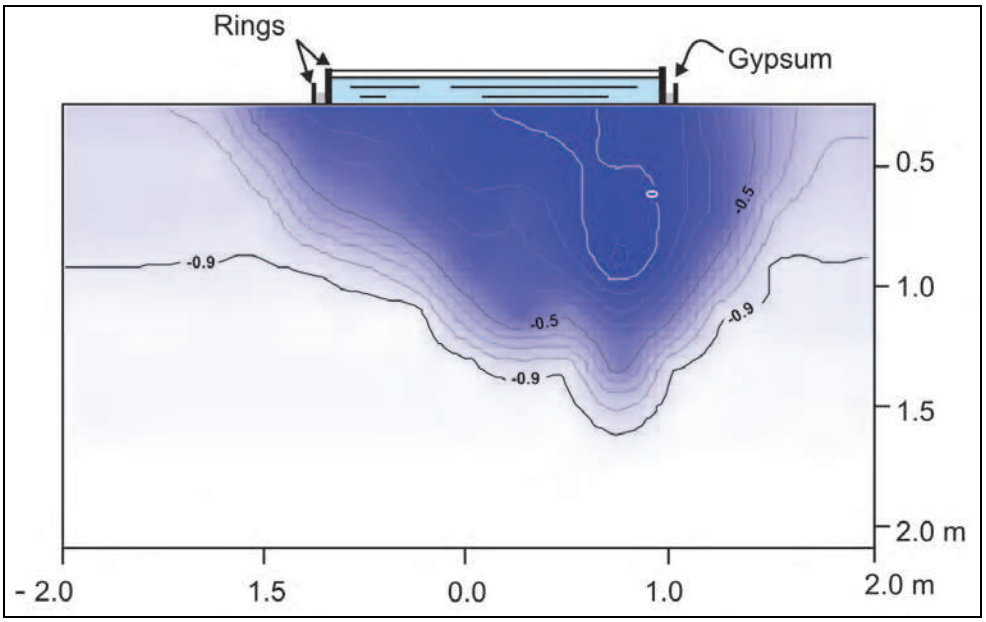


Fig. 7. Best selected model simulation output in order to fit the shape of the wetting front at t = 80 min. Contour lines represent model output expressed as matric potential (m) in the fracture.

It should be noted that the former conductivity value is very similar to the field-saturated conductivity obtained by the ring infiltrometer in test #1 (0.67 m $d^{-1}$). In contrast, the field-saturated conductivity (0.054 m $d^{-1}$) derived from test #2, where the limestone outcrop had no visible fractures, is close to the value (0.02 m $d^{-1}$) obtained by laboratory tests on the rock matrix of the Murge limestone (Borgia et al., 2002). The above comparison supports the field-saturated hydraulic conductivity values obtained using the large ring infiltrometers. Simultaneous electrical subsurface measurements, inverted by using the Res2Dinv software, also show a difference in behavior between the two tests as a consequence of the water infiltration during the tests (Fig. 8). Before the infiltrometer tests ($t \leq 0$ min), the subsurface resistivity was above 500 Ωm at the first site and more than 2,000 Ωm at the second site. In test #1, the low resistivity area, below 150 Ωm, was visualized after 80 minutes to about 1.5 m of depth; similar results were obtained for the electrode arrays in the perpendicular direction. The low resistivity zones can be related qualitatively to fractured rock with high water content and moderate salinity. The same resistivity value was visualized at shallower depth, at the same time, during test #2 than the previous test. In fact, in the last case, it is not possible to evaluate the depth of wetting front from a quantitative point of view, because the

resolution of the resistivity images depends on the electrode spacing. As rule of thumb, a structure or object in the subsurface, having dimensions less than the electrode spacing, cannot be defined clearly. For both tests the electrical resistivity measurements confirmed the effectiveness of the ring sealing, showing that the water infiltrated from within the ring and not from outside (Fig. 8). Additionally, electrical resistivity imaging highlights not only that the water reached different depths in the two infiltrometer tests, but also that its variable redistribution, within the investigated vertical plane, results from the structural characteristics of the limestone outcrop. As expected, in test #1, the deepening of the level of the low resistivity anomaly associated with the infiltration of moderately saline water was much greater than in test #2, and was, in fact, consistent with the different number and size of the fractures observed visually in the limestone.

### 4.2 Calcarenite

The results of the field experiments carried out on the calcarenitic layer of the vadose zone outcropping at the bottom of the quarry, are shown in Figures 9 and 10. The Figures show the infiltration data and the electrical resistivity images, respectively. In order to interpret the results of constant head infiltrometer test we have plotted the infiltration rate, $q = dI / dt$ , versus time, t, as shown it the graph of Figure 9a. The value of q, initially decreases rapidly with time and then approaches a constant value. Practically, the rate of infiltration falls, starting from very high values at the beginning of the test when the subsurface is in an unsaturated condition, up to a value of $9x10^{-4} \pm 0.0001$ cm/s (i.e. between 0.86 $md^{-1}$ to 0.69 $md^{-1}$), when the rock is in quasi-saturated condition. For the studied calcarenite, this value of the infiltration rate, obtained by considering the horizontal asymptote of the curve, was reached after about 2 hours from the start of the infiltration, depending upon the water content of the rock at the beginning of the test. This value should be approximately equal to the field-saturated hydraulic conductivity value, $K_{fs.}$ Again for the falling head infiltrometer test, equation (5) was considered. In this case a λ value equal to 0.01 m was used for the calcarenite, taking into account that the sensitivity of conductivity calculations to the value of λ is small (Nimmo et al., 2009), and that Elrick et al. (1989) proposed a λ value of about 0.08 m suitable for most soils with structural development, a value of 0.03 m for gravelly soils, and 0.25 m for fine-textured soil without macropores. Figure 9b shows the plot of the effective infiltration length (right-hand side of equation (5), except the variable t) vs. time and the slope of this regression line is a convenient calculation of $K_{fs}$. The graph shows how the $K_{fs}$ values decrease during the infiltration test, from the highest value of $1.22x10^{-3}$ cm/s (i.e. 1.05 $md^{-1}$), at the start of the test, until the lowest of $5.61x10^{-4}$ cm/s (i.e. 0.48 $md^{-1}$) at the end of the infiltration, with an average value of $8.13x10^{-4}$ cm/s (i.e. 0.77 $md^{-1}$). This last value is consistent with the quasi-steady infiltration rate value, obtained from the constant head test (Fig. 9a). The variability of the field-saturated hydraulic conductivity, $K_{fs}$, observed in Figure 9b depends on the change in water content with the time during the experiment: higher $K_{fs}$ values are obtained in the initially dry rock than in that wet. In fact, the soil water content during the test has been considered an important factor that affects the $K_{fs}$ value of the experimental area (Bagarello & Sgroi, 2007). In order to have a rough estimation of the wetting front depth, a porosity value of about 0.4 was considered. Using this value of porosity and the high infiltration rate of about 4 cm/s for the first 20 minutes of the constant head test, it was estimated that the wetting front should reach a depth of about 20 cm, while up to the end of the falling head test, by considering

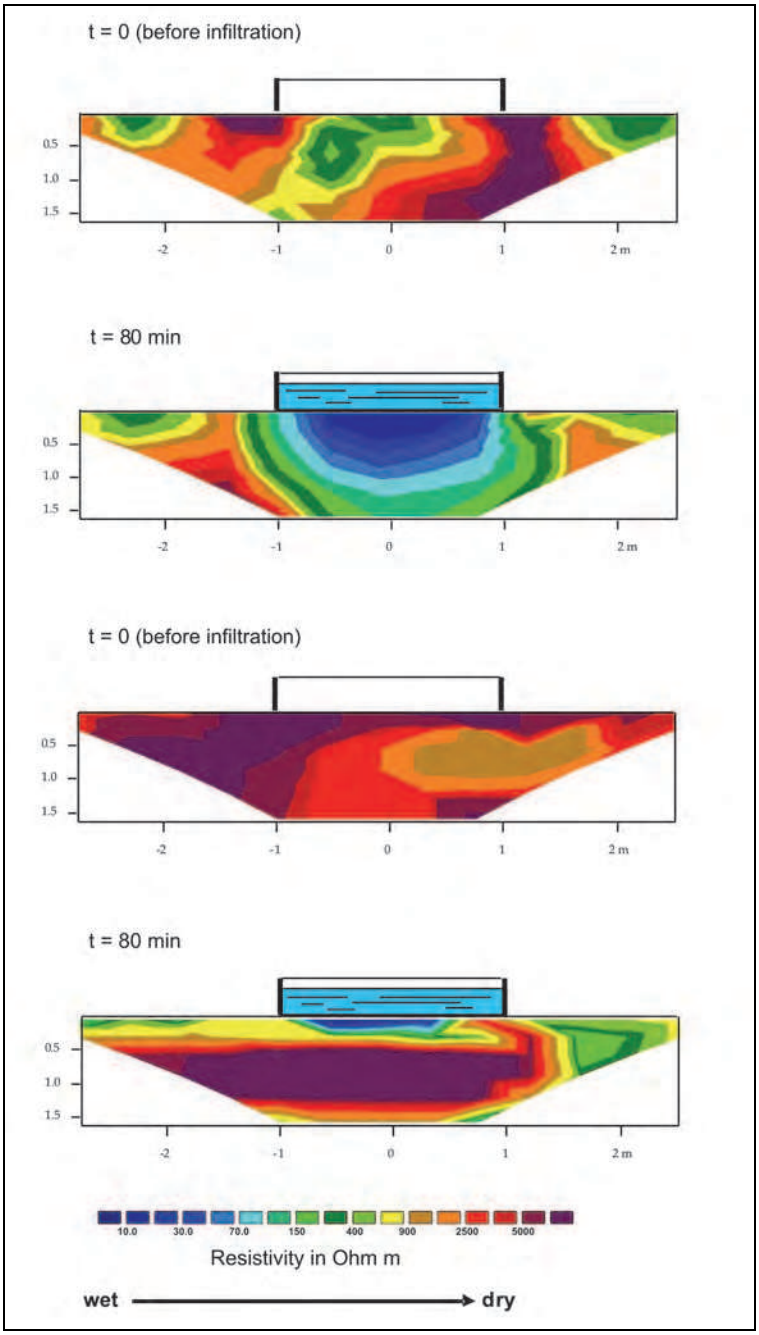


Fig. 8. Electrical resistity profiles during test # 1 and # 2, before (t = 0 min) and during (t = 80 min) water infiltration tests at the Altamura site.

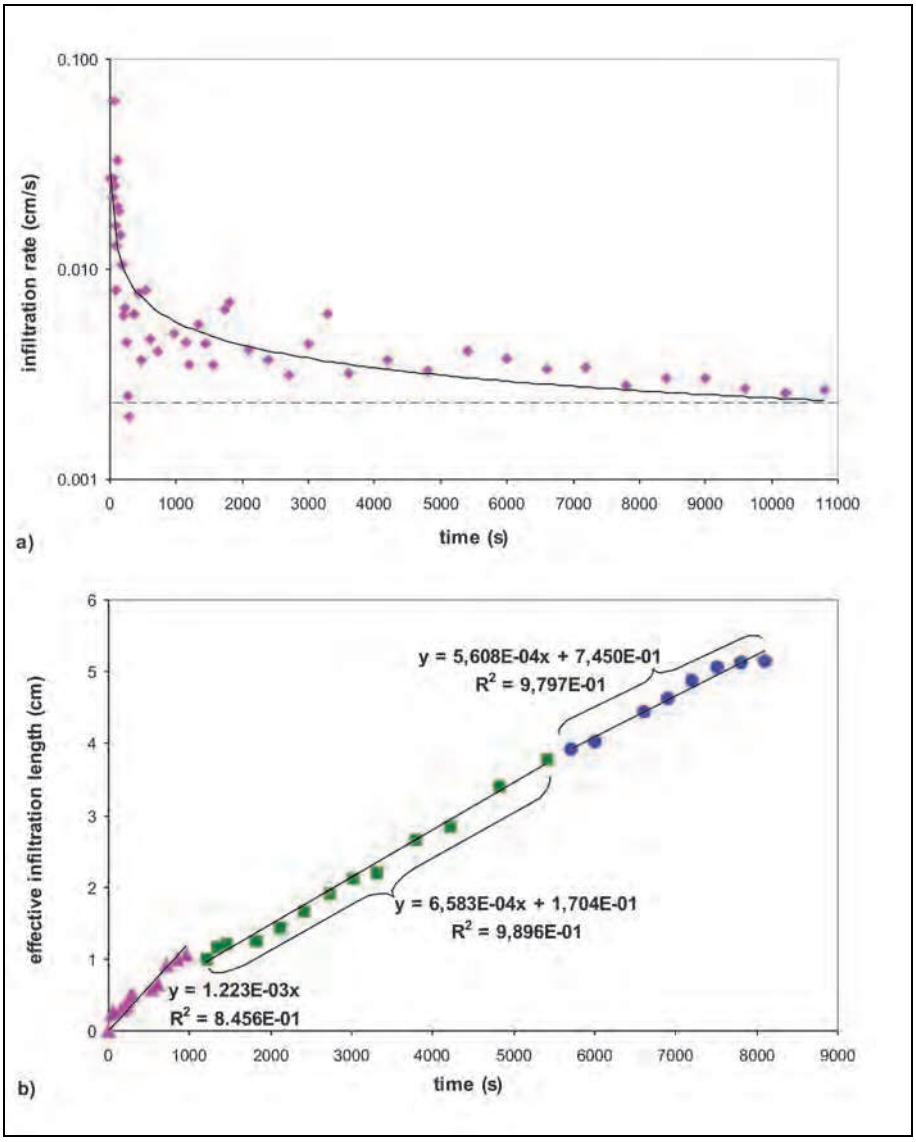


Fig. 9. Test at the San Pancrazio site: a) constant head infiltration test – infiltration rate versus time; b) falling head infiltration test – effective infiltration length versus time.

an average infiltration rate of about $9x10^{-4}$ cm/s, it should only deepen by about another 6 cm. Obviously, this so small a difference in depth that it is not perceptible in the chronological sequences of electrical resistivity images (Fig. 10). Knowing that the shallow aquifer is at 12 m below the bottom of the quarry where the waste was disposed, it was estimated that the time required for the pollutants to reach the shallow groundwater is just over 15 days. Concerning the results of the electrical resistivity surveys, using time-lapse

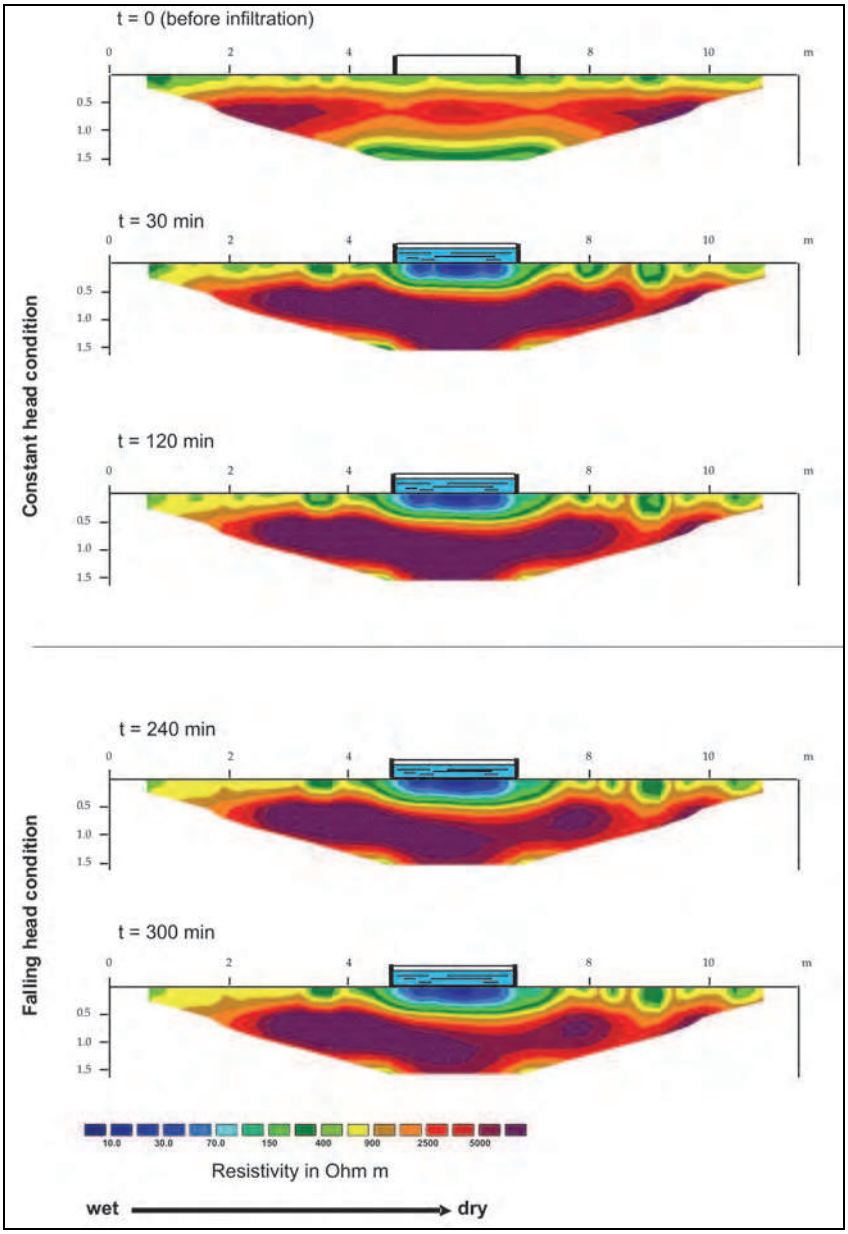


Fig. 10. Electrical resistivity profiles during infiltration test at the San Pancrazio site – profile 1.

techniques, 2-D resistivity images were obtained for different acquisition times. The electrical resistivity images showed no significant differences between the two perpendicular directions (Fig. 10). The first two profiles on the top of Figure 10, measured

before starting water infiltration ($t \leq 0$ min) and characterized by resistivity values above 1,000 Ωm, represent the profiles with which to compare the following profiles, in order to monitor the water flux in the subsurface. The images from the constant head test show that the wetting front (resistivity values around 60 Ωm) deepens in the first 20 minutes of the experiment, much more than in the following 4.5 hours, up to the end of the test. These results are consistent with the high values of infiltration rate, correspondent to the initial part of the constant head test. The images related to the sequences of the electrical resistivity profiles, acquired during the falling head test (Fig. 10), are similar to the last profile of the constant head condition, such as we expected by considering that the field-saturated hydraulic conductivity values, obtained from the tests under the different conditions, are similar.

## 5. Conclusion

The large ring infiltrometer, coupled with subsurface electrical resistivity measurements, described in this chapter, has proved to be a simple and inexpensive field tool, capable of evaluating the field-saturated hydraulic conductivity of rock formations, even if it requires numerical elaboration supported by mathematical models, in certain conditions. It is designed to be installed directly on an outcrop of both hard and soft rock, and easily constructed on site with inexpensive, lightweight materials, and has an adjustable diameter. These characteristics improve the versatility of the infiltrometer method and its adaptability to various geological conditions. Thus it expands the potential for exploring field-hydraulic conductivity of rocks, which until now has been investigated more frequently in laboratories, mainly because of the practical difficulties involved in field investigations. Simultaneous electrical resistivity measurements are used to monitor the subsurface water infiltration instead of humidity sensors or tensiometers, thus sidestepping the difficulty of inserting probes into the rock. Further technical difficulties, related to the installation in the field of the large ring infiltrometer, were solved using non-commercially available equipment during the on-site installation procedure. Specifically, the setup of the experimental apparatus requires the hollowing out of a furrow in which to install the ring and seal it to the rock surface with gypsum. Otherwise, if the field conditions of the infiltration area are very heterogeneous, consisting of different media, e.g. rock and soil, an infiltrometer made of two concentric rings is suggested in order to improve the hydraulic packing during the water infiltration test. In this case the continuity between the ring infiltrometer wall and the rock-soil surface is obtained by filling the space between the external and internal rings with gypsum, up to a height of about 2.0 cm,to create a seal. Thus the second ring improves the gypsum seal of the first ring with the ground, overcoming the challenge presented by the presence of different media along the edge of the ring. The efficacy of the seal of ring infiltrometer with soil/rock surfaces was confirmed by the simultaneous electrical resistivity measurements that show the deepening and spreading of the water during the infiltration tests. The time required for the installation was about two hours and the water volume used for each infiltration test was about 0.5 $m^3$ for the limestone, and about 0.3 $m^3$ for calcarenite, depending on the local rock permeability. On the whole, the field- hydraulic conductivity data obtained from the infiltrometer tests (0.67 m $d^{-1}$ and 0.054 m $d^{-1}$, for tests #1 and #2 on limestone, respectively, and 0.77 m $d^{-1}$ for calcarenite) are consistent with the nature of the rocks tested and are corroborated by laboratory measurements carried out by other authors (Quarto & Schiavone, 1994; Borgia et

al., 2002). The difference between the field-saturated hydraulic conductivity values obtained by the infiltration tests, highlights the difference of the outcrops studied, owing to the different geological formations characterized from variable heterogeneity degree (number and size of fractures). The possibility of building a ring with a large adjustable diameter on site, has the advantage of including fractures and other features of the rock in order to obtain field-saturated hydraulic conductivity data at a more representative scale of measurements, with negligible border effects. The proposed installation procedure of a large ring infiltrometer on rocky outcrops extends the possibility of performing field infiltrometer tests on rocks that would, previously, have been very difficult to test. Simultaneous subsurface electrical resistivity imaging, using time-lapse techniques, is a useful indicator of water infiltration/redistribution. Moreover, the electrical resistivity survey provides evidence that the conductivity structure is confined under the ring infiltrometer, confirming that the apparatus works well in order to minimize the lateral lack of water, without having losses along the edge of the ring, allowing the acquisition of accurate and representative experimental data. On the other hand, it is important to highlight that the geophysical inversion model used, Res2Dinv, has not been able to represent the heterogeneities and anisotropies of the heterogeneous system, such as fractured or karstic rocks. This consideration encourages further research and study in order to define new algorithms able to derive real images closer to the real subsurface features than now, starting from the electrical resistivity measurements of heterogeneous systems. Using the simplified equation for determining the field-saturated hydraulic conductivity from the experimental data of falling head infiltrometer tests, it is demonstrated that the proposed method works well, in different cases, proving it is a good tool to know how quickly the water moves through the unsaturated zone in real field conditions.

## 6. Acknowledgment

The work was partially funded by the Italian Government (Regional Autority), which is gratefully acknowledged. We thank Costantino Masciopinto for his collaboration in modelling on fractured systems and for his fruitful cooperation during the field experiments. We also thank Rita Masciale and Francesco De Benedictis for their support for the field work and for their comments during the preparation and revision of this document.

## 7. References

Archie, G.E. (1942). The Electrical Resistivity Log as an Aid in Determining Some Reservoir Characteristics. *Petroleum Transactions of AIME*, Vol. 146, pp. 54–62.

Bagarello, V. & Sgroi, A. (2007). Using the Simplified Falling Head Technique to Detect Temporal Changes in Field-Saturated Hydraulic Conductivity at the Surface of a Sandy Loam Soil. *Soil & Tillage Research,* Vol. 94, pp. 283–294.

Baumhardt, R.L., Lascano, R.J. & Evett, S.R. (2000). Soil Material, Temperature, and Salinity Effects on Calibration of Multisensor Capacitance Probes. *Soil Science Society of America Journal*, Vol.64, pp. 1940-1946.

Binley, A.M., Cassiani, G., Middleton, R. & Winship, P. (2002). Vadose Zone Flow Model Parameterization Using Cross-Borehole Radar and Resistivity Imaging. *Journal of Hydrology*, Vol. 267 (3-4), pp. 147-159.

Bogena, H.R., Huisman, J.A., Oberdosrster, C.A. & Vereecken, H. (2007). Evaluation of a Low-Cost Soil Water Content Sensor for Wireless Network Application. *Journal of Hydrology*, Vol. 344, pp. 32-42.

Borgia, G.C., Bortolotti. V. & Masciopinto, C. (2002). Valutazione del Contributo della Porosità Effettiva alla Trasmissività di Acquiferi Fratturati con Tecniche di Laboratorio e di Campo (Evaluation of Effective Porosity Contribution to the Transmissivity of Fractured Aquifer Using Laboratory and Field Techniques). *IGEA, Groundwater Geoengineering*, Vol. 17, pp. 31-43.

Cassiani, G., Bruno, V., Villa, A., Fusi, N. & Binley, A.M. (2006). A Saline Tracer Test Monitored via Time-Lapse Surface Electrical Resistivity Tomography. *Journal of Applied Geophysics*, Vol. 59, pp. 244-259.

Castiglione, P., Shouse, P.J., Mohanty, B., Hudson, D. & van Genucthen, M.Th. (2005). Improved Tension Infiltrometer for Measuring Low Flow Rates in Unsaturated Fractured Rock. *Vadose Zone Journal*, Vol. 4, pp. 885-890.

Ciaranfi, N., Pieri, P. & Ricchetti, G. (1988). Note alla Carta Geologica delle Murge e del Salento (Puglia Centro-Meridionale) (Notes on the Geological Map of Murge and Salento (Central-Southern Puglia). *Memorie.della Società Geologica Italiana,* Vol. 41, pp. 449-460.

Dahlin, T. (2001). The Development of DC Resistivity Imaging Techniques. *Computers & Geosciences,* Vol. 27, pp. 1019-1029.

Dahlin, T. (1996). 2-D Resistivity Surveying for Environmental and Engineering Applications. *First Break*, Vol. 14 (7), pp. 275–283.

Daily, W., Ramirez, A., LaBrecque, D. & Nitao, J. (1992). Electrical Resistivity Tomography of Vadose Water Movement. *Water Resources Research*, Vol. 28(5), pp. 1429-1442.

de Gennes, P.G., Brochard-Wyart, F. & Quéré, D. (2002). Capillary and Wetting Phenomena: Drops, Bubbles, Pearls, Waves. Springer. ISBN 0-387-00592-7.

deGroot-Hedlin, C. & Constable, S. (1990). Occam's Inversion to Generate Smooth, Two-Dimensional Models from Magnetotelluric Data. *Geophysics*, Vol. 55, pp. 1613-1624.

Deiana, R., Cassiani, G., Kemna, A., Villa, A., Bruno, V. & Bagliani, A. (2007). An Experiment of Non-Invasive Characterization of the Vadose Zone via Water Injection and Cross-Hole Time-Lapse Geophysical Monitoring. *Near Surface Geophysics*, Vol. 5, pp. 183-194.

Edwards, L.S. (1977). A Modified Pseudosection for Resistivity and Induced-Polarization. *Geophysics,* Vol. 42, pp. 1020-1036.

Elrick, D.E, Reynolds, W.D. & Tan, K.A. (1989). Hydraulic Conductivity Measurements in the Unsaturated Zone Using Improved Well Analyses. *Ground Water Monitoring Review*, Vol. 9, pp. 184-193.

Griffiths, D.H. & Barker, R.D. (1993). Two-Dimensional Resistivity Imaging and Modelling in Areas of Complex Geology. *Journal of Applied Geophysics*, Vol.29, pp. 211-226.

Jones, S.B. & Or, D. (2004). Frequency Domain Analysis for Extending Time Domain Reflectometry Water Content Measurement in Highly Saline Soils. *Soil Science Society of America Journal*, Vol. 68, pp. 1568–1577, 2004.

Kizito, F., Campbell, C.G., Cobos, D.R., Teare, B.L., Carter, B. & Hopmans, J. W. (2008). Frequency, Electrical Conductivity and Temperature Analysis of a Low-Cost Capacitance Soil Moisture Sensor. *Journal of Hydrology*, Vol. 352, pp. 367-378.

Lai, J. & Ren, L. (2007). Assessing the Size Dependency of Measured Hydraulic Conductivity Using Double-Ring Infiltrometers and Numerical Simulation. *Soil Science Society of American Journal,* Vol. 71, pp. 1667-1675.

Leeds-Harrison, P.B., Youngs, E.G. & Uddin, B. (1994). A Device for Determining the Sorptivity of Soil Aggregates. *European Journal of Soil Science,* Vol. 45, pp. 269-272.

Loke, M.H. (2001). *A tutorial on 2-D and 3-D electrical imaging surveys.* Avalaible from www.geoelectrical.com.

Loke, M.H. & Barker, R.D. (1996). Rapid Least-Squares Inversion of Apparent Resistivity Pseudosections by a Quasi-Newton Method. *Geophysical Prospecting,* Vol. 44, pp. 131-152.

Masbrucha, K. & Ferré, T.P.A. (2003) A Time-Domaine Transmission Method for Determining the Dependence of the Dialectric Permittivity on Volumetric Water Content. An Application to Municipal Landifills. *Vadose Zone Journal,* Vol. 2, pp. 186-192.

Masciopinto, C. (2005). Pumping-Well Data for Conditioning the Realization of the Fracture Aperture Field in Groundwater Flow Models. *Journal of Hydrology*, Vol. 309 (1-4), pp. 210-228.

Masciopinto, C. & Benedini, M. (1999). Unsaturated Flow in Fractures with Anisotropic Variable Apertures, *Proceedings of XXVIII IAHR - AIRH Congress*, Graz, Austria, August 23–27, 1999.

Nimmo, J.R., Schmidt, K.S., Perkins, K.S. & Stock J.D. (2009) Rapid Measurement of Field-Saturated Hydraulic Conductivity for Areal Characterization. *Vadose Zone Journal*, Vol 8, pp.142-149.

Pape, H., Clauser, C. & Iffland, J. (1999). Permeability Prediction Based on Fractal Pore-Space Geometry. *Geophysics*, Vol. 64(5), pp. 1447-1460.

Pruess, K. & Tsang, Y.W. (1990). On Two-Phase Relative Permeability and Capillary Pressure on Rough-Walled Rock Fractures. *Water Resources Research*, Vol. 26(9), pp. 1915-1926.

Quarto, R. & Schiavone, D. (1994). Hydrogeological Implications of the Resistivity Distribution Inferred from Electrical Prospecting Data from the Apulian Carbonate Platform. *Journal of Hydrology,* Vol. 154, pp. 219-244.

Reynolds, J. M. (1998). *An Introduction to Applied and Environmental Geophysics*, Wiley, (Ed.) John Wiley and Sons, ISBN 0-471-9555-8, New York.

Reynolds, W.D., Elrick, D.E. & Young, E.G. (2002). Ring or Cylinder Infiltrometers (Vadose Zone), In: *Method of Soil Analysis,* J.K. Dane & G.C. Topp, (Eds.), pp. 818-826, Soil Science Society of America, Inc., ISBN 0-89118-841-X Madison, Wisconsin, USA.

Robinson, D.A., Jones, S.B., Wraith, J. M., Or, D. & Friedman, S. P. (2003). A Review of Advances in Dielectric and Electrical Conductivity Measurement in Soils Using Time Domain Reflectometry. *Vadose Zone Journal*, Vol. 2, pp. 444– 475.

Seyfried, M.S., & Murdock, M.D. (2004). Measurement of Soil Water Content with a 50-Mhz Soil Dielectric Sensor. *Soil Science Society of America Journal,* Vol. 68(2), pp. 394-403.

Swartzendruber, D., & Olson, T.C. (1961). Model Study of the Duble Ring Infiltrometer as Affected by Depth of Wetting and Particle Size. *Soil Science,* Vol. 92, pp. 219-225.

Telford, W.M., Geldart, L.P. & Sheriff, R.E. (1990). *Applied Geophysics* (2nd edition), Cambridge University Press, ISBN 0-521-33938-3, Cambridge.

Youngs, E.G., Spoor, G. & Goodall, G.R. (1996). Infiltration from Surface Ponds into Soils Overlying a Very Permeable Substratum. *Journal of Hydrology*, Vol. 186, pp. 327–334.

White, P.A. (1988). Measurement of Ground-Water Parameters Using Salt-Water Injection and Surface Resistivity. *Ground Water*, Vol. 26, pp. 179–186.


**Hydraulic Conductivity - Issues, Determination and Applications**

Edited by Prof. Lakshmanan Elango

ISBN 978-953-307-288-3
Hard cover, 434 pages
**Publisher** InTech
**Published online** 23, November, 2011
**Published in print edition** November, 2011

There are several books on broad aspects of hydrogeology, groundwater hydrology and geohydrology, which do not discuss in detail on the intrigues of hydraulic conductivity elaborately. However, this book on Hydraulic Conductivity presents comprehensive reviews of new measurements and numerical techniques for estimating hydraulic conductivity. This is achieved by the chapters written by various experts in this field of research into a number of clustered themes covering different aspects of hydraulic conductivity. The sections in the book are: Hydraulic conductivity and its importance, Hydraulic conductivity and plant systems, Determination by mathematical and laboratory methods, Determination by field techniques and Modelling and hydraulic conductivity. Each of these sections of the book includes chapters highlighting the salient aspects and most of these chapters explain the facts with the help of some case studies. Thus this book has a good mix of chapters dealing with various and vital aspects of hydraulic conductivity from various authors of different countries.

**How to reference**

In order to correctly reference this scholarly work, feel free to copy and paste the following:

Maria Clementina Caputo and Lorenzo De Carlo (2011). Field Measurement of Hydraulic Conductivity of Rocks, Hydraulic Conductivity - Issues, Determination and Applications, Prof. Lakshmanan Elango (Ed.), ISBN: 978-953-307-288-3, InTech, Available from: http://www.intechopen.com/books/hydraulic-conductivity-issues-determination-and-applications/field-measurement-of-hydraulic-conductivity-of-rocks

INTECH
open science | open minds

**InTech Europe**
University Campus STeP Ri
Slavka Krautzeka 83/A
51000 Rijeka, Croatia
Phone: +385 (51) 770 447
Fax: +385 (51) 686 166
www.intechopen.com

**InTech China**
Unit 405, Office Block, Hotel Equatorial Shanghai
No.65, Yan An Road (West), Shanghai, 200040, China
中国上海市延安西路65号上海国际贵都大饭店办公楼405单元
Phone: +86-21-62489820
Fax: +86-21-62489821